Available online at www.sciencedirect.com
ScienceDirect
Journal of the European Ceramic Society 30 (2010) 1911–1917
www.elsevier.com/locate/jeurceramsoc

Stability of rare earth oxides in a moist environment at elevated temperatures—Experimental and thermodynamic studies Part II: Comparison of the rare earth oxides

Emilie Courcot [a,*], Francis Rebillat [a,*], Francis Teyssandier [a], Caroline Louchet-Pouillerie [b]

[a] *Université de Bordeaux, Laboratoire des Composites ThermoStructuraux, 3 Allée de la Boétie, 33600 Pessac, France*
[b] *Snecma Propulsion Solide, Groupe Safran, Zi Les Cinq Chemins, 33185 Le Haillan, France*

Received 10 July 2009; received in revised form 4 February 2010; accepted 8 February 2010
Available online 29 March 2010

Abstract

Volatilisation tests enabled to quantify the stability of different rare earth sesquioxides, RE_2O_3 (where RE = Sc, Dy, Er, Yb) and to understand the corrosion process. These tests were carried out at temperatures ranging from 1000 to 1400 °C in moist air with 50 kPa of water at atmospheric pressure, under a flowing gas velocity of 5 cm s^{-1}. Besides the volatilisation rate, the nature of the volatile gaseous species was determined. The proposed experimental method allowed too to assess the Gibbs free energy of formation of these gaseous volatile species. Finally, the stability of each rare earth oxide under a moist environment at high temperature was compared.

Keywords: Corrosion; Chemical properties; Refractories; Rare earth oxide; Thermodynamics

1. Introduction

Rare earth sesquioxides (RE_2O_3) may be assumed as the most common oxides of rare earth elements since these compounds are known for all of them. They present a great scientific and technologic interest because of their high chemical stability and their attractive chemical and physical properties. These materials are, for example, often used as dopants in thermal barrier coatings.[1] In Table 1, some properties of these oxides are reported.[2,3] All the rare earth oxides melt in the range from 2573 K and 2773 K. Depending on the melting temperature and atomic number of the lanthanide element, two groups have to be distinguished[4]: the first one, Ceric group, includes the oxides from La_2O_3 to Gd_2O_3, and the second, the Yttric one, the oxides from Dy_2O_3 to Lu_2O_3. Y_2O_3 and Sc_2O_3 belong to this last group. The melting point decreases when the rare earth ionic radius increases. The values of density follow the similar trend (Table 1).

Concerning their structural properties, these oxides may present a polymorphism; five distinct crystalline types have been identified.[4] These polymorphic modifications are usually labelled with some letters: A, H for hexagonal, B for monoclinic, C and X for cubic. The domain of existence of each phase depends on temperature and on the rare earth ionic radius (Fig. 1). The A, B and C structures are commonly found at temperatures below 2000 °C, whereas X and H at temperatures above 2000 °C. Only rare earth elements with ionic radii values owning to the middle range are able to form all the five allotropic phases. For the lighter lanthanides, the C form may be metastable, whereas for the heavier than Gd_2O_3 and for Y_2O_3, the C form is stable from room temperature to high temperature. Lu_2O_3 and Sc_2O_3 have no polymorphs and present a transition directly from C-type solid to the molten state.

With regard to the physical properties, it is interesting to note that oxides with a similar structure and density have, for example, similar values of specific heat, or refraction index.[5] Moreover, rare earth oxides have a low electric conductivity. Here, heavier is the rare earth, lower is the conductivity.[6]

Concerning the thermodynamic properties, the rare earth sesquioxides have been commonly assumed to vaporize congruently with a composition in agreement with almost the

* Corresponding authors. Tel.: +33 556 84 47 31; fax: +33 556 84 12 25.
E-mail addresses: courcot@lcts.u-bordeaux1.fr (E. Courcot), rebillat@lcts.u-bordeaux1.fr (F. Rebillat).

0955-2219/$ – see front matter © 2010 Elsevier Ltd. All rights reserved.
doi:10.1016/j.jeurceramsoc.2010.02.012

Table 1
Stuctural properties of RE_2O_3.

	La_2O_3	Pr_2O_3	Nd_2O_3	Sm_2O_3	Eu_2O_3	Gd_2O_3	Sc_2O_3	Y_2O_3	Dy_2O_3	Ho_2O_3	Er_2O_3	Yb_2O_3	Lu_2O_3
Family	Ceric						Yttric						
r_{ionic} (Å)	1.06	1.01	0.99	0.96	0.95	0.94	0.73	0.89	0.91	0.89	0.88	0.86	8.84
Melting point (K)	2578	2573	2593	2608	2623	2693	2758	2723	2691	2688	2691	2708	2763
Density	6.57	7.06	7.33	7.75	7.95	8.30	3.84	5.03	8.17	8.42	8.66	9.22	9.43
Structure	Hexagonal: P_{-3ml}			Monoclinic C_{2m}			Cubic: I_{a-2}						

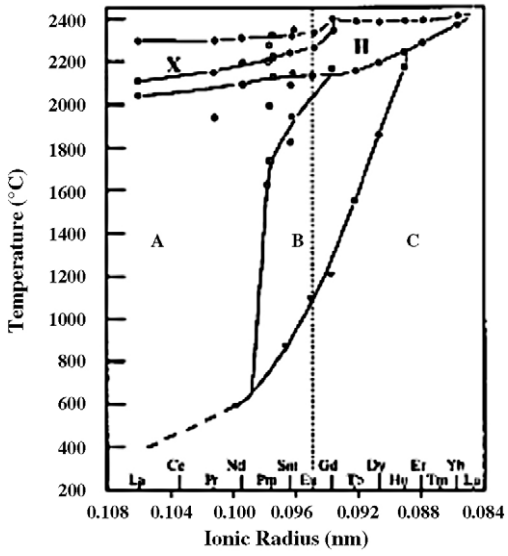

Fig. 1. Existence domains of the RE_2O_3 polymorphs in function of temperature and of rare earth ionic radius.[4]

stoechiometry ratio.[4] The gaseous rare earth oxide species of the general formulas RO, R_2O, RO_2 and R_2O_2 have been observed.[7] It has been shown that the gaseous monoxides of the lighter lanthanides were considerably more stable than those of heavy lanthanides. This feature can be explained by the fact that the gaseous atoms ($f^n s^2$) in the lighter lanthanide atoms are considerably more accessible than those in the heavier lanthanide atoms to bond effectively to oxygen.[4]

In this work, some rare earth sesquioxides belonging to the yttric group are considered: Sc_2O_3, Dy_2O_3, Er_2O_3 and Yb_2O_3. Their volatilisation rates under a moist environment were measured in order to quantify their stability, to identify the nature of the gaseous volatile hydroxides and to deduce their Gibbs free energy of formation.

2. Experimental approach

Powders (Sc_2O_3, Neyco, 99.99% and Dy_2O_3, Er_2O_3 and Yb_2O_3, Chempur, 99.9%) were mixed and compacted under an unidirectional pressure of 0.5 MPa during 10 min. Pellets were heat treated at 1300 °C during 5 h under ambient air for desorption and sintering. The porosity was around 25%.

Actually, moisture provokes an enhanced degradation of materials by reaction with the oxides leading to the volatilisation of hydroxides $RE(OH)_3$ or oxy-hydroxides REO(OH) (Eqs. (1)–(2)):

$$RE_2O_3 + 3H_2O \rightarrow 2RE(OH)_3 \quad (1)$$

$$RE_2O_3 + H_2O \rightarrow 2REOOH \quad (2)$$

In order to quantify the volatility of oxides and identify the nature of the main gaseous species formed, a methodology based on weight loss measurements was developed by Courcot et al.[8] The main steps are schematized in Fig. 2. The volatilisation tests are carried out at temperatures between 1000 and 1400 °C, in a moist air (water vapour partial pressure up to 68 kPa, 100 kPa total pressure with air to complete), with a gas

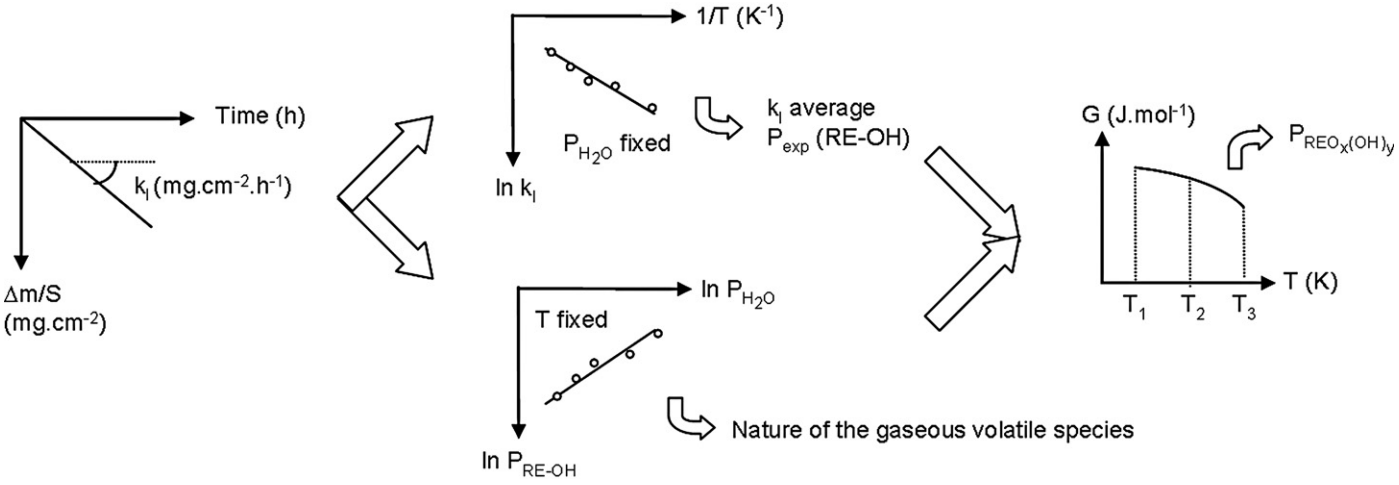

Fig. 2. Experimental approach used for the assessment of the hydroxide thermodynamic data.

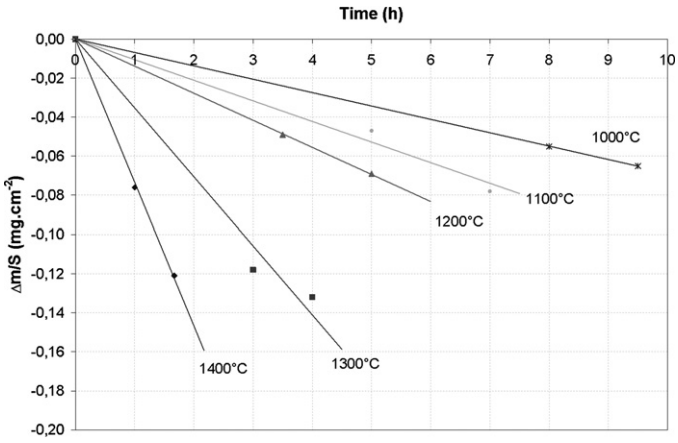

Fig. 3. Weight changes during volatilisation of Sc_2O_3 at different temperatures, under corrosion with 50 kPa H_2O, at P_{atm} with $v_{gas} = 5\ cm\ s^{-1}$.

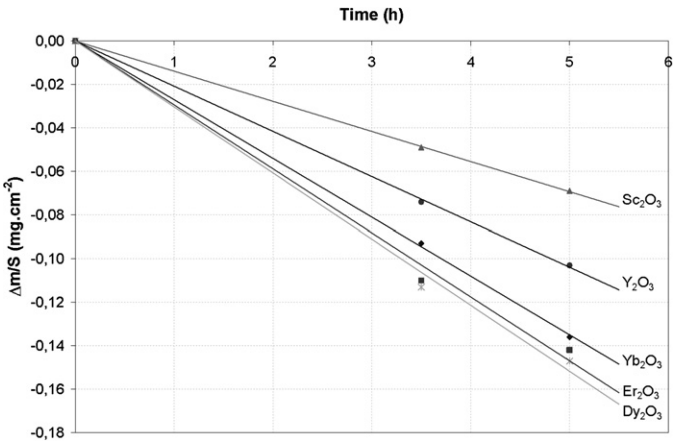

Fig. 4. Weight changes during volatilisation of RE_2O_3 at 1200 °C, under corrosion with 50 kPa H_2O, at P_{atm} with $v_{gas} = 5\ cm\ s^{-1}$.

velocity of 5 cm s^{-1} (in the cold zone of the furnace) during times between 1.5 h and 20 h on oxide pellets, desorbed at 1300 °C during 5 h in ambient air. Each weight measurement is conducted on a separated pellet in order to avoid any problems with REAG ($RE_3Al_5O_{12}$) or REAM ($RE_4Al_2O_9$) formation by reaction with $Al(OH)_3$ impurities coming from the furnace tube, as discussed in a previous paper.[8] Data were considered as accurate after similar results obtained from three independent experiments.

3. Results and discussion

In the literature, there are no information concerning the stability of rare earth sesquioxides in a corrosive atmosphere and the nature of the gaseous volatile species. Consequently, to get these data, experiments have to be carried out by varying either the temperature, or the water partial pressure.

3.1. Determination of the activation energy of the volatilisation process

First, during the volatilisation tests, the water partial pressure was fixed to 50 kPa and the temperature varies from 1000 °C to 1400 °C. The variations of the ratio between the weight change and the surface of the pellet as a function of time are shown for Sc_2O_3 in the range of temperatures between 1000 and 1400 °C in Fig. 3 and for all considered rare earth oxides at 1200 °C in Fig. 4. These results are compared to Y_2O_3.[8] The weight loss is linear with time and increases with temperature. The volatilisation rates k_l deduced from the slope of the linear curves are gathered in Table 2. The interfacial reaction process is thermally activated and the Arrhenius graph $\ln k_l$ in function of $1/T$ is plotted (Fig. 5). Rare earth oxides appear to have two volatilisation mechanisms, with a transition temperature between 1100 °C and 1300 °C. This transition is in fact characterized by a rupture in the linear evolution of the Arrhenius law. The first mechanism is valuable at low temperatures, and the second one at high temperatures. Thus, it can be supposed that: two gaseous species exist and the main gaseous species formed may differ respectively between the two temperature domains.

The values of the activation energy and the pre-exponential term are reported in Table 3. At high temperatures, the activation energy is higher than that of volatilisation of silica under the $Si(OH)_4$ form ($61 \pm 8\ kJ\ mol^{-1}$).[9,10] At low temperatures, the activation energy is close to that of silica. The low values of uncertainties associated to these parameters allow clearly distinguishing the behaviour of the different rare earth oxides. Even if all considered oxides belong to the yttric group, it is possible to distinguish two oxide types: the d^1 family and the f^n one. In fact, Sc_2O_3 and Y_2O_3 have similar values of activation energy and preexponential term. Concerning Dy_2O_3, Er_2O_3 and Yb_2O_3, their activation energy and their preexponential term increase with the ionic radius of the rare earth element. Consequently, the values of the activation energy and of the preexponential term can be related to the chemical bond in the oxide structure and respectively to the number of the electrons for each rare earth.

Besides the fact that a relation between the activation energy, the preexponential term and the ionic radius was found, this study enabled to conclude that rare earth oxides belonging to the yttric group have two mechanisms of volatilisation. This

Table 2
Volatilisation rates of RE_2O_3 in a moist environment at different temperatures ($P_{H_2O} = 50$ kPa, $P_{tot} = P_{atm}$, $v_{gaz} = 5\ cm\ s^{-1}$).

k_l (mg $cm^{-2}\ h^{-1}$)	1000 °C	1100 °C	1200 °C	1300 °C	1400 °C
Y_2O_3	0.0122 ± 0.0003	0.0162 ± 0.0001	0.0208 ± 0.0003	0.051 ± 0.001	0 12 ± 0 01
Sc_2O_3	0.0069 ± 0.0001	0.0105 ± 0.0006	0.0138 ± 0.0001	0.037 ± 0.002	0.074 ± 0.001
Dy_2O_3	0.0112 ± 0.0007	0.019 ± 0.004	0.030 ± 0.002	0.058 ± 0.009	0.15 ± 0.03
Er_2O_3	0.0127 ± 0.0007	0.019 ± 0.001	0.0294 ± 0.0009	0.05 ± 0.02	0.12 ± 0.01
Yb_2O_3	0.0074 ± 0.0002	0.012 ± 0.002	0.0270 ± 0.0004	0.050 ± 0.002	0.11 ± 0.01

Table 3
Kinetic parameters (Arrhenius law) of the rare earth oxide volatilisation in a moist atmosphere ($P_{H_2O} = 50$ kPa, $P_{tot} = P_{atm}$, $v_{gaz} = 5$ cm s^{-1}).

	Y_2O_3	Sc_2O_3	Dy_2O_3	Er_2O_3	Yb_2O_3
r_{ionic} (Å)	0.89	0.73	0.91	0.88	0.86
E_a^{LT} (kJ mol^{-1})	41 ± 1	54 ± 1	77 ± 1	06 ± 1	(727)
K_o^{LT} (mg cm^{-2} h^{-1})	0.506 ± 0.002	1.2 ± 0.1	17.2 ± 0.2	6.1 ± 0.2	(7.086)
$T_{transition}$ (°C)	~1200	~1200	1265	1240	<1100
E_a^{HT} (kJ mol^{-1})	175 ± 5	172.3 ± 1	215 ± 1	187 ± 5	137 ± 3
K_o^{HT} (mg cm^{-2} h^{-1})	3.3E+04±1E+04	1.8E+04±0.2E+04	8.0E+05±0.1E+05	8E+04±1E+04	2.0E+03±0.5E+03

feature has now to be related to the nature of different gaseous volatile hydroxides formed.

3.2. Identification of the nature of the gaseous hydroxide species

The nature of the different gaseous species can be identified by modifying the water partial pressure between different corrosion tests at fixed temperatures. In fact the (oxy-) hydroxide partial pressures depend on the water partial pressures (Eq. (3)). According to the stoechiometric ratio in Eqs. (1) and (2), the plot of ln P(RE-OH) vs ln $P(H_2O)$ would yield a linear graph with a slope of 1.5 if the main species were $RE(OH)_3$ and 0.5 if REOOH.

$$K = \frac{P_{\text{RE-OH}}}{P_{H_2O}^{y}} \Rightarrow \ln P_{\text{RE-OH}} = \ln K + y \ln P_{H_2O} \quad (3)$$

The (oxy-)hydroxide partial pressures are calculated from the values of volatilisation rates (Eq. (4)). This extraction of the partial pressures of the formed gaseous species allows taking accurately into account the low experimental variations of gas velocity (induced with a change of gas mixture). It can be mentioned that this equation is valuable whatever the nature of the hydroxide formed since the stoechiometric ratio before the formed gaseous species for one molecule of solid oxide volatilized in Eqs. (1) and (2) remains constant (=2).

$$k_l = v_{gas} \times 3.6 \times M_{RE_2O_3} \times \frac{1}{2} \times \frac{P_{\text{RE-OH}}}{R \times T_{amb}};$$
$$\text{where } P_{\text{RE-OH}} = P_{RE(OH)_3} + P_{\text{REOOH}} \quad (4)$$

where k_l is the volatilisation rate (mg cm^{-2} h^{-1}), v_{gas} is the gas flow velocity at room temperature (cm s^{-1}), $M_{RE_2O_3}$ is the molar weight of RE_2O_3 (g mol^{-1}), 2 is the stoechiometry ratio before the formed gaseous species in Eq. (1) or (2), $P_{\text{RE-OH}}$ is the sum of the volatile gaseous species partial pressures (Pa), R is the ideal gas constant (=8.314 J mol^{-1} K^{-1}) and T_{amb} is the ambient temperature (296 K).

Therefore, volatilisation tests were carried out at 1000, 1200 and 1400 °C in air with different water partial pressures (ranging from 17 kPa to 68 kPa) under atmospheric pressure, with a gas flow velocity of 5 cm s^{-1} in the cold zone of the furnace

At each temperature, a different value of slope is extracted (Table 4). At 1400 °C, an average value around 1.4 has to be correlated to the favoured formation of $RE(OH)_3$. At 1000 °C, according to the slopes, the predominant gaseous species was REOOH. At 1200 °C, the nature of the gaseous species depends on the rare earth oxides. Actually these results on different volatilisation mechanisms are in agreement with the Arrhenius plot (Fig. 5). Formation of REOOH is expected to take place at low temperatures, whereas $RE(OH)_3$ should be the high temperature hydroxide species. The increasing of the slopes with the temperature is indicative of an increasing proportion of $RE(OH)_3$ formed at the expense of REOOH.

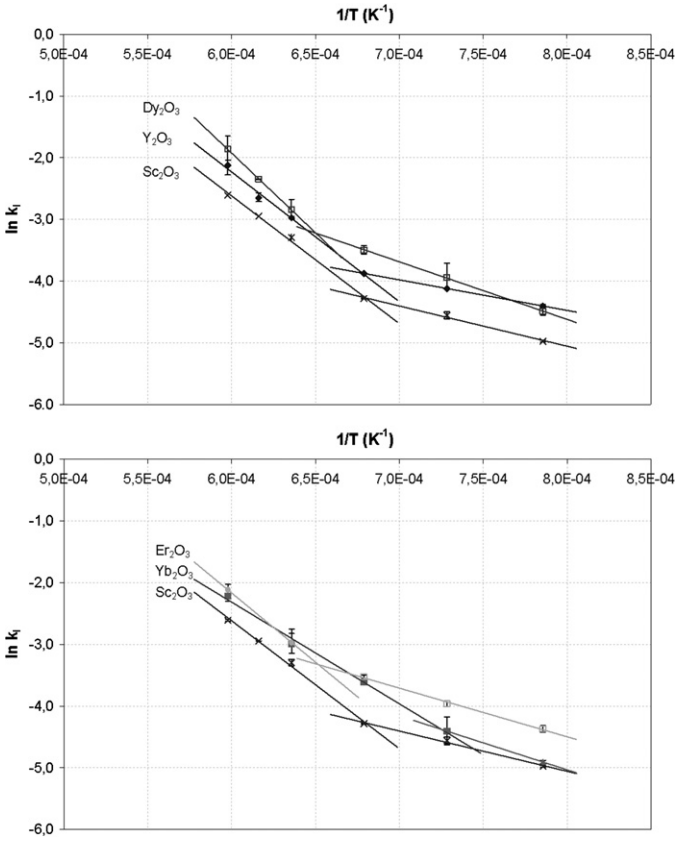

Fig. 5. Arrhenius graph concerning the volatilisation of the rare earth oxide under a moist environment at high temperature ($P_{H_2O} = 50$ kPa, $P_{tot} = P_{atm}$, $v_{gaz} = 5$ cm s^{-1}; k_l in mg cm^{-2} h^{-1}) (if not visible, uncertainties are hidden in the size of the dots).

3.3. Assessment of thermodynamic data

In order to assess the thermodynamic parameters of REOOH and $RE(OH)_3$, an overview of all gaseous species containing rare earth and oxygen formed has to be done and their

Table 4
Identification of the nature of the gaseous volatile species in relation with the reaction order associated to water.

Slope of $P_{RE\text{-}OH}$ vs P_{H_2O}	Y_2O_3	Sc_2O_3	Dy_2O_3	Er_2O_3	Yb_2O_3
1000 °C	$0.87 \pm 0.01 \rightarrow YOOH + Y(OH)_3$	$0.86 \pm 0.01 \rightarrow ScOOH + Sc(OH)_3$	$0.95 \pm 0.10 \rightarrow DyOOH + Dy(OH)_3$	$0.94 \pm 0.10 \rightarrow ErOOH + Er(OH)_3$	$1.06 \pm 0.15 \rightarrow Yb(OH)_3 + YbOOH$
1200 °C	$1.19 \pm 0.02 \rightarrow Y(OH)_3 + YOOH$	$0.86 \pm 0.10 \rightarrow ScOOH + sc(OH)_3$	$0.94 \pm 0.10 \rightarrow DyOOH + Dy(OH)_3$	$0.97 \pm 0.15 \rightarrow ErOOH + Er(OH)_3$	$1.24 \pm 0.05 \rightarrow Yb(OH)_3 + YbOOH$
1400 °C	$1.46 \pm 0.03 \rightarrow Y(OH)_3$	$1.20 \pm 0.14 \rightarrow Sc(OH)_3 + ScOOH$	$1.53 \pm 0.10 \rightarrow Dy(OH)_3$	$1.32 \pm 0.05 \rightarrow Er(OH)_3 + ErOOH$	$1.44 \pm 0.04 \rightarrow Yb(OH)_3$

Table 5
Thermodynamic data of formation of RE_2O_3,[11] $RE(OH)_3$ and REOOH ($\Delta G = a + bT + cT\ln T + dT^2 + eT^{-1} + fT^{-2}$).

ΔG (J mol^{-1})	a	b	c	d	e	f
Sc_2O_3	−1.9554720000E+06	7.5148930000E+02	−1.2843000000E+01	−4.2270000000E−03	1.8260000000E+06	−5.2000000000E+07
$Sc(OH)_3$	−9.5941361840E+05	−5.5103840000E+02	–	1.0399999999E−02	–	–
ScOOH	1.2545564653E+06	−3.5206022000E+03	–	1.2857000000E+00		–
Dy_2O_3	−1.9023160000E+06	6.7913130000E+02	−1.2259300000E+02	−6.9710000000E−03	5.9000000000E+01	4.0000000000E+07
$Dy(OH)_3$	−2.8540086498E+05	−1.3510733334E+03	–	2.3166666667E−01	–	–
DyOOH	1.4002661958E+05	−1.7510220500E+03	–	5.6767500000E−01	–	–
Er_2O_3	−1.9397140000E+06	6.5265620000E+02	−1.1921600000E+02	−58890000000E−03	4.2800000000E+02	2.0000000000E+07
$Er(OH)_3$	−1.1690949084E+06	−3.1073840000E+02	_	−7.9600000000E−02	–	–
ErOOH	3.1089014325E+05	−2.0678435000E+03	–	7.0025000000E−01	–	–
Yb_2O_3	−1.8535110000E+06	7.0275020000E+02	−1.2382100000E+02	−4.5670000000E−03	0.0000000000E+00	5.0000000000E+07
$Yb(OH)_3$	−9.3768945200E+05	−5.6595200000E+02		1.1999999999E−02	–	
YbOOH	−1.2178038039E+06	2.1209860000E+02	–	−1.0910000000E−01	–	–
Y_2O_3	−1.8535110000E+06	7.0275020000E+02	−1.2382100000E+02	−4.5670000000E−03	0.0000000000E+00	5.0000000000E+07
$Y(OH)_3$	−9.3768945200E+05	−5.6595200000E+02	–	1.1999999999E−02	–	–
YOOH	−1.2178038039E+06	2.1209860000E+02	–	−1.0910000000E−01	–	–

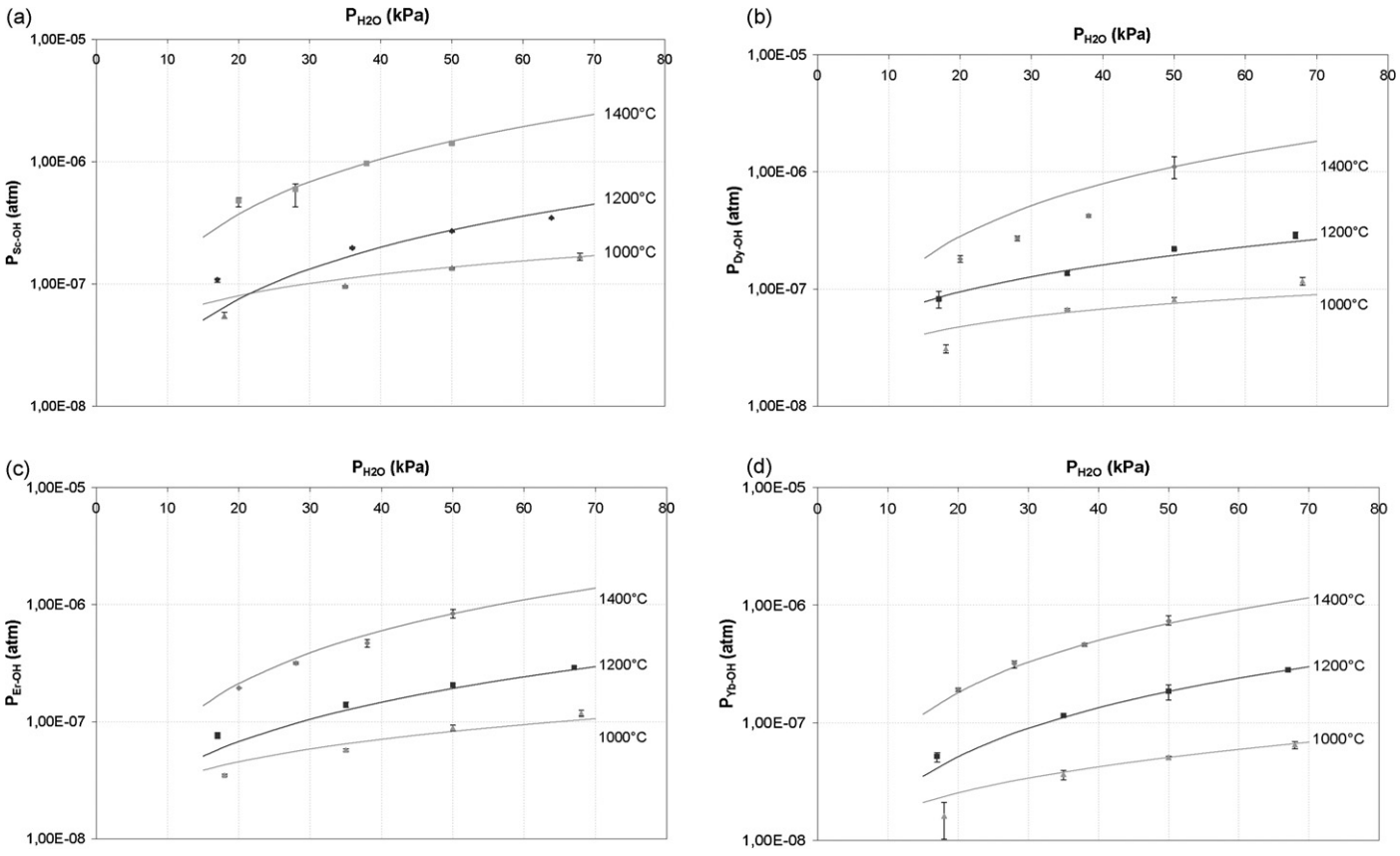

Fig. 6. Comparison of experimental (symbols) and calculated (curves) hydroxides pressures using the Gibbs free energies of a: $Sc(OH)_3$ and ScOOH formation; b: $Dy(OH)_3$ and DyOOH formation; c: $Er(OH)_3$ and ErOOH formation and d: $Yb(OH)_3$ and YbOOH formation ($P_{tot} = P_{atm}$, $v_{gaz} = 5\,cm\,s^{-1}$) (if not visible, uncertainties are hidden in the size of the dots).

associated thermodynamic data are compiled. This compilation is extended to the solid phase, RE_2O_3. As far as our knowledge, no data on oxide gaseous species are available for temperatures between 1000 and 1400 °C. In fact, available data are valuable from 2000 K.[4] The thermodynamic parameters of RE_2O_3 are well documented[11] and those used in this study are compiled in Table 5.

The assessment of the thermodynamic data of each gaseous species is based on the calculations of their partial pressures. These partial pressures are estimated from the volatilisation Arrhenius law obtained at atmospheric pressure (Fig. 5) with a water partial pressure of 50 kPa using the expression of the average volatilisation rate (Eq. (4)).

In our study, two cases can be distinguished: the first one at high temperature (>1100 °C to 1300 °C), where $RE(OH)_3$ is the predominant species and the second one at low temperatures, where a mixture of REOOH and $RE(OH)_3$ is obtained.

In a first step, the Gibbs free energy of formation of $RE(OH)_3$ is determined in the high temperature domain. The variations of Gibbs free energy of $Sc(OH)_3$ and $Yb(OH)_3$ formation between 1300 and 1400 °C was determined according to the above-described procedure from measurements carried out at 1300 °C, 1350 °C and 1400 °C. This methodology can not be applied for $Dy(OH)_3$ and $Er(OH)_3$, since the transition between the two volatilisation mechanisms occurs at 1300 °C. Consequently, partial pressures at 1450 °C have been only evaluated from the Arrhenius law and Eq. (4). The values of Gibbs free energy of $Dy(OH)_3$ and $Er(OH)_3$ formation between 1350 °C and 1450 °C have been determined as described previously. In all cases to describe the variations of the Gibbs free energy of formation, a temperature dependant equation was deduced. Extrapolation of this equation in the low temperature domain allowed to calculate the partial pressures of $RE(OH)_3$ below 1300 °C, when this gaseous species is the minor one. Thus, the partial pressures of REOOH were deduced (Eq. (5)). The same procedure was applied at 1000, 1100 and 1200 °C (and 1300 °C for Dy_2O_3 and Er_2O_3) and a temperature dependant equation describing the variations of the Gibbs free energy of formation of REOOH was obtained in the low temperature domain.

$$P_{exp} = P_{RE(OH)_3} + P_{REO(OH)} \quad (5)$$

The variations of Gibbs free energy of formation of $RE(OH)_3$ and REOOH are listed in Table 5.

In order to check that the thermodynamic parameters are correct for different water partial pressures, the sum of partial pressures of hydroxide species (Eq. (5)) obtained for P_{H_2O} comprised between 17 kPa and 68 kPa were compared with thermodynamic calculations (Fig. 6). The calculated curve is compared with the experimental points. The good agreement between the latter points and the curve going through validates the assessed thermodynamic data.

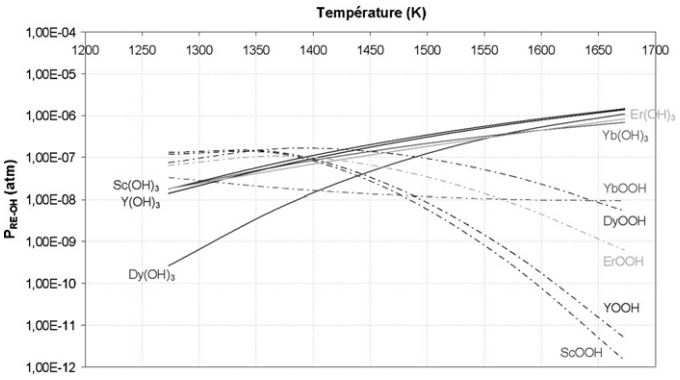

Fig. 7. Comparison of hydroxide partial pressures (where $P_{RE\text{-}OH}$ is either $P_{RE(OH)_3}$ or P_{REOOH}) in equilibrium with each solid oxide RE_2O_3 (P_{H_2O} = 50 kPa, $P_{tot} = P_{atm}$).

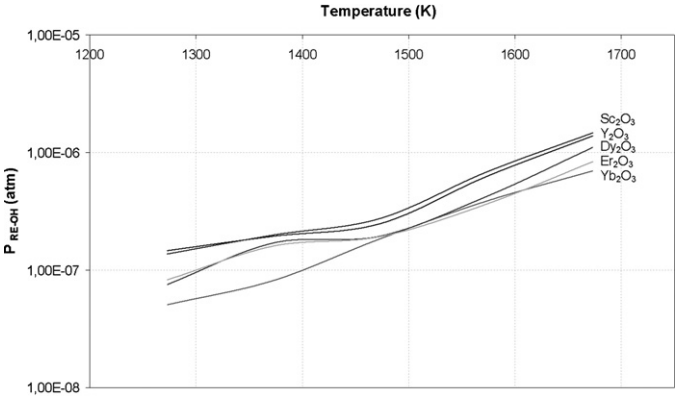

Fig. 8. Comparison of hydroxide partial pressures ($P_{RE\text{-}OH} = P_{RE(OH)_3} + P_{REOOH}$) in equilibrium with each solid oxide RE_2O_3 ($P_{H_2O} = 50$ kPa, $P_{tot} = P_{atm}$).

To reinforce this validation, partial pressures of $RE(OH)_3$ and REOOH at the equilibrium over RE_2O_3 were calculated for a water partial pressure of 50 kPa (Fig. 7). Their variations are in agreement with the hypothesis done on the predominant existence domains of each hydroxide species. When the values of volatilisation rates of rare earth oxides are compared between themselves, lanthanide oxides appear to be more stable under a moist atmosphere at high temperatures than Y_2O_3 or Sc_2O_3. This is in agreement with the values of activation energy, which is higher for lanthanides. The most stable oxide seems to be Yb_2O_3, since the partial pressures of $Yb(OH)_3$ and YbOOH are the lowest (Fig. 8).

4. Conclusions

Rare earth sesquioxide volatilisation under a moist environment is characterized by two mechanisms. The first one is valuable at low temperatures, where REOOH is the predominant species formed by reaction of moisture with RE_2O_3. This reaction is characterized by a low activation energy, value close to that of silica. At high temperatures, a second mechanism leads to the predominant formation of $RE(OH)_3$. In this case, the activation energy is twice or three times higher than that at low temperatures. A relation is highlighted between the ionic radius and the activation energy or the preexponential term (in the Arrhenius law). For lanthanides, higher is the ionic radius, higher are the activation energy and the preexponential term. For Sc_2O_3 and Y_2O_3, similar values of activation energy and preexponential term are obtained. Further, Gibbs free energy of REOOH and $RE(OH)_3$ formation are assessed, and their partial pressures are calculated. The relative stabilities of rare earth sesquioxides are compared and Yb_2O_3 seems to be the most stable rare earth oxide under a moist environment. Future works consist in quantify the stability of diverse rare earth silicates by using these data. In fact, the rare earth silicates based EBCs have shown good recession resistance in regard to Si_3N_4, or mainly SiO_2, alone as a protection.[12] These developed EBCs have been proved the effectiveness by actual engine durability. This can be explained by the bonding between SiO_2 and another refractory oxide, which allows decreasing the activity of silica in silicates, thus enhancing the thermal and chemical stability of SiO_2.

Acknowledgement

This work has been supported by the French Ministry of Education and Research through a grant given to E. Courcot.

References

1. Ma W, Mack D, Malzbender J, Vaβen R, Stöver D. Yb_2O_3 and Gd_2O_3 doped strontium zirconate for thermal barrier coatings. *J Eur Ceram Soc* 2008;**28**:3071–81.
2. Lide DR. *Handbook of chemistry and physics*. 71st ed. Boston: CRC Press; 1990.
3. Bruker AXS GmbH, Diffracplus, PDF Maint; 2000.
4. Adachi G-Y, Imanaka M. The binary rare earth oxides. *Chem Rev* 1998;**98**:1479–514.
5. Fornarini L, Conde JC, Alvani C, Olevano D, Chiussi S. Experimental determination of La_2O_3 thermal conductivity and its application to the thermal analysis of a-Ge/La_2O_3/c-Si laser annealing. *Thin Solid Films* 2008;**516**:7400–5.
6. Rao GVS, Ramdas S, Mehtora PN, Rao CNR. Electrical transport in rare-earth oxides. *J Solid State Chem* 1970;**2**:377–84.
7. Gingerich KA. Molecular species in high temperature vaporization. *Curr Top Mater Sci Amsterdam* 1980;**6**:345 [chapter 5].
8. Courcot E, Rebillat F, Teyssandier F, Louchet-Pouillerie C. Stability of rare earth oxides in a moist environment at elevated temperatures—Experimental and thermodynamic studies. Part I: The way to assess thermodynamic data from volatilisation rates. *J Eur Ceram Soc* 2010;**30**(9):1903–9.
9. Hashimoto A. The effect of H_2O gas on volatilities of planet-forming major elements. I. Experimental determination of thermodynamic properties of Ca-, Al-, and Si-hydroxide gas molecules and its application to the solar nebula. *Geochim Cosmochim Acta* 1992;**56**:511–32.
10. Opila EJ, Hann RE. Paralinear oxidation of CVD SiC in water vapor. *J Am Ceram Soc* 1997;**80**:197–205.
11. Zinkevich M. Thermodynamics of rare earth sesquioxides. *Prog Mater Sci* 2007;**52**:597–647.
12. Fukudome T, Tsuruzono S, Tatsumi T, Ichikawa Y, Hisamatsu T, Yuri I. Development of silicon nitride components for gas turbine. *Key Eng Mater* 2005;**287**:10–5.